Dalton Transactions

PAPER

View Article Online
View Journal | View Issue

Check for updates

Cite this: *Dalton Trans.*, 2019, **48**, 15668

Tetranuclear oxido-bridged thorium(IV) clusters obtained using tridentate Schiff bases†‡

Sokratis T. Tsantis,[a] Aimilia Lagou-Rekka,[a] Konstantis F. Konidaris,[a,b] Catherine P. Raptopoulou,[c] Vlasoula Bekiari,*[b] Vassilis Psycharis*[c] and Spyros P. Perlepes*[a,d]

Thorium(IV) complexes are currently attracting intense attention from inorganic chemists due to the development of liquid-fluoride thorium reactors and the fact that thorium(IV) is often used as a model system for the study of the more radioactive Np(IV) and Pu(IV). Schiff-base complexes of tetravalent actinides are useful for the development of new separation strategies in nuclear fuel processing and nuclear waste management. Thorium(IV)–Schiff base complexes find applications in the colorimetric detection of this toxic metal ion and the construction of fluorescent on/off sensors for Th(IV) exploiting the ligand-based light emission of its complexes. Clusters of Th(IV) with hydroxide, oxide or peroxide bridges are also relevant to the environmental and geological chemistry of this metal ion. The reactions between Th$(NO_3)_4{\cdot}5H_2O$ and *N*-salicylidene-*o*-aminophenol (LH_2) and *N*-salicylidene-*o*-amino-4-methylphenol ($L'H_2$) in MeCN have provided access to complexes $[Th_4O(NO_3)_2(LH)_2(L)_5]$ (**1**) and $[Th_4O(NO_3)_2(L'H)_2(L')_5]$ (**2**) in moderate yields. The structures of **1**·4MeCN and **2**·2.4 MeCN have been determined by single-crystal X-ray crystallography. The complexes have similar molecular structures possessing the $\{Th_4(\mu_4\text{-}O)(\mu\text{-}OR')_8\}$ core that contains the extremely rare $\{Th_4(\mu_4\text{-}O)\}$ unit. The four Th^{IV} atoms are arranged at the vertexes of a distorted tetrahedron with a central $\mu_4\text{-}O^{2-}$ ion bonded to each metal ion. The H atom of one of the acidic –OH groups of each 3.21 LH^- or $L'H^-$ ligand is located on the imine nitrogen atom, thus blocking its coordination. The Th^{IV} centres are also held together by one 3.221 L^{2-} or $(L')^{2-}$ group and four 2.211 L^{2-} or $(L')^{2-}$ ligands. The metal ions adopt three different coordination numbers (8, 9, and 10) with a total of four coordination geometries (triangular dodecahedral, muffin, biaugmented trigonal prismatic, and sphenocorona). A variety of H-bonding interactions create 1D chains and 2D layers in the crystal structures of **1**·4 MeCN and **2**·2.4 MeCN, respectively. The structures of the complexes are compared with those of the uranyl complexes with the same or similar ligands. Solid-state and IR data are discussed in terms of the coordination mode of the organic ligands and the nitrato groups. ^{1}H NMR data suggest that solid-state structures are not retained in DMSO. The solid complexes emit green light at room temperature upon excitation at 400 nm, the emission being ligand-centered.

Received 5th August 2019,
Accepted 29th August 2019

DOI: 10.1039/c9dt03189h

rsc.li/dalton

Open Access Article. Published on 02 2019. Downloaded on 2025/7/31 07:35:32.
This article is licensed under a Creative Commons Attribution 3.0 Unported Licence.

Introduction

The ions of early actinide (An) elements are unique in inorganic chemistry in that they combine large radii and lanthanide (Ln) ions' Lewis acidity with the potential for remarkable covalency (due to greater f-orbital radial extension for An *vs.* Ln ions), and due to the fact that they can achieve a broad range of oxidation states (mainly for U, Np and Pu).[1–3]

These characteristics provide An complexes with some special reactivity profiles. Thorium was discovered in 1829 by the famous chemist Jöns Jacob Berzelius and owes its name to Thor, the Scandinavian god of thunder and war.[4] Natural Th is radioactive, but many of its current uses exploit its chemical, rather than its nuclear, features. Thorium is the first true An element and has an empty 5f orbital, its outer electronic con-

[a]*Department of Chemistry, University of Patras, 26504 Patras, Greece. E-mail: perlepes@patreas.upatras.gr; Tel: +30 2610 996730*
[b]*School of Agriculture Sciences, University of Patras, 30200 Messolonghi, Greece. E-mail: mpekiari@teimes.gr; Tel: +30 26310 58260*
[c]*Institute of Nanoscience and Nanotechnology, NCSR "Demokritos", 15310 Aghia Paraskevi Attikis, Greece. E-mail: v.psycharis@inn.demokritos.gr; Tel: +30 210 6503346*
[d]*Foundation for Research and Technology-Hellas (FORTH), Institute of Chemical Engineering Sciences (ICE-HT), Platani, P.O. Box 144, 26504 Patras, Greece*

†Dedicated to Professor Annie K. Powell on the occasion of her 60th birthday: a great scientist, an excellent mentor for the Patras group, a fantastic personality and a precious friend.

‡Electronic supplementary information (ESI) available: Structural plots and spectroscopic data. Cifs and checkcifs for the two complexes. CCDC 1945475 and 1945476. For ESI and crystallographic data in CIF or other electronic format see DOI: 10.1039/c9dt03189h

This journal is © The Royal Society of Chemistry 2019

Open Access Article. Published on 02 2019. Downloaded on 2025/7/31 07:35:32.
This article is licensed under a Creative Commons Attribution 3.0 Unported Licence.

figuration being $6d^2 5f^2$; therefore, Th(IV) is the most stable and almost exclusive oxidation state.[5]

There has been a renaissance in the coordination and material chemistry of Th(IV) for the last 5 years or so.[1,6–21] There are several reasons for this. The main reason is that Th is widely considered to be the next generation nuclear fuel as the development of Liquid-Fluoride Thorium Reactors (LFTRs) comes closer to commercialization.[5,6,22,23] India is keen on using thorium as the nuclear fuel (this country has approximately 30% of the world's thorium reserves) and plans to produce one third of its electricity from thorium by 2050.[5] The production of thorium is usually achieved by the separation of Th^{4+} from Ln^{3+} ions, since the main thorium production mineral is monazite which contains the ions of 4f metals; mining is based on liquid–liquid extraction with organic ligands,[24,25] hence the importance of the Th(IV) coordination chemistry. There is also intense interest for the development of new efficient solid absorbents for the selective extraction of Th^{4+} ions from 4f-metal ions.[16]

Other research areas of Th(IV) chemistry that are currently attracting attention from inorganic chemists include the incorporation of this diamagnetic ion into coordination clusters instead of the paramagnetic U(IV) to elucidate the magnetic exchange interactions between the d-metal ions in d/U^{IV} complexes,[26] its interaction with ionic liquids to model the aspects of the extraction of An ions from radioactive feeds (a process of great relevance in nuclear fuel cycle activities),[13] the understanding of Th(IV) peroxide chemistry,[8,14] the study of the solution and solid-state structural chemistry of Th(IV) hydrolysis and condensation products,[9,11] the stabilization of novel secondary building units in Th(IV)-based Metal–Organic Frameworks (MOFs),[15,19] the characterization of complexes with very high coordination numbers (up to 14) and unusual coordination geometry,[7] the in-depth investigation of the thermodynamic and electronic properties of heterometallic An^z/Th^{IV} (z = various) and An/Th^{IV}/3d-metal ion MOFs with "structural memory"[20] and the progress in compounds with Th(IV)-ligand multiple bonds.[12]

Schiff bases have been used extensively as ligands with metals across the Periodic table.[27] These molecules are attractive for their easy and high-yield preparation, their solubility in a variety of organic solvents, and their ability to stabilize metals in various oxidation states and control behaviour of metal ions during catalysis;[28–33] in addition, their steric and electronic properties are highly tunable. The coordination chemistry of the *trans*-UO_2^{2+} ion (uranyl ion) with Schiff bases is a well explored area.[34–38] However, tetravalent actinides, An(IV), have been little studied. Schiff-base complexes of An(IV) are of great utility for the development of new An separation strategies in nuclear fuel processing and nuclear waste management.[39] Restricting the discussion to Th(IV), its Schiff-base complexes (which are scarce in the literature[40–42] are closely related to the development of colorimetric detection of this metal ion and applications in real-time samples,[43] to the construction of on/off sensors for Th(IV) exploiting the ligand-based light emission of its complexes,[44] and to the study of

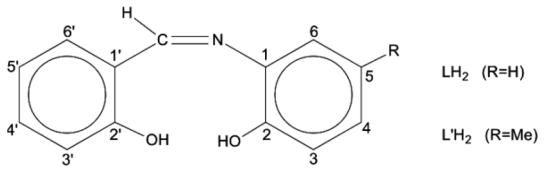

Scheme 1 General structural formula of the tridentate ONO Schiff bases used in the present work and their abbreviations.

Th(IV) reactions with the derivatives of vitamin B_6 as a means to understand the assimilation of this metal ion and other heavy nuclei by living organisms and its acute toxicological effects.[45] A drawback associated with tetradentate dianionic O,N,N,O ligands of the salen^{2-}-type is their planarity and charge. The valence completion of An(IV), *e.g.* Th(IV), requires often two ligands per metal ion and this may result in hindered reactivity due to steric effects. Once the bis-Schiff-base complex is isolated, no further ligand-substitution is possible and the redox chemistry of redox-active An^{IV} centres, *e.g.* U^{VI}, is rather poor.[41] Therefore, the interest in this area has shifted to potentially dianionic, tridentate Schiff bases. Two such ligands are *N*-salicylidene-*o*-aminophenol [or *N*-(2-hydroxyphenyl)salicylaldimine; LH_2 in Scheme 1] and *N*-salicylidene-*o*-amino-4-methylphenol [or *N*-(2-hydroxy-5-methylphenyl)-salicylaldimine; $L'H_2$ in Scheme 1]. The number 4 in the first (empirical) name of $L'H_2$ (which is in disagreement with the numbering code in Scheme 1) is used because its origin is from the name of the starting material, *i.e.*, 4-methyl-2-aminophenol used for the synthesis of $L'H_2$.[46]

Upon deprotonation of one or both –OH groups of LH_2 and $L'H_2$, each negatively charged phenoxido atom can bridge two or three metal ions favouring cluster formation, while the position of the imino N atom simultaneously assures the formation of chelating rings that can lead to thermodynamic stability of the products in solution. The anions of the ligands have been widely used in main group-,[47] 3d-,[48–51] 4f-[52,53] and mixed 3d/4f-metal[54] chemistry by our group and other scientists, with emphasis on the magnetic properties of the complexes. The use of LH_2 and $L'H_2$ in 5f-metal chemistry is negligible (*vide infra*). No Th(IV) complexes have been prepared with these ligands.

Having all the above mentioned in mind, and given our interest in the chemistry of An ions[55–57] and in the coordination chemistry of LH_2 and its derivatives,[46,48–52] we report herein the reactions of $Th(NO_3)_4{\cdot}5H_2O$ with LH_2 and $L'H_2$, and the full characterization of the interesting products.

Experimental section

Materials, physical and spectroscopic measurements

All manipulations were performed under aerobic conditions using materials (reagent grade) and solvents as received. The free ligands LH_2 and $L'H_2$ were synthesized by the reactions of salicylaldehyde, and 2-aminophenol and 4-methyl-2-amino-

Open Access Article. Published on 02 2019. Downloaded on 2025/7/31 07:35:32.
This article is licensed under a Creative Commons Attribution 3.0 Unported Licence.

phenol, respectively, in refluxing MeOH or EtOH using published procedures;[58–60] the yields were in the 75–80% range. Their purity was checked by microanalyses and ^{1}H NMR spectra. *Caution!* Natural thorium (primary isotope ^{232}Th) is a weak α-emitter (4.012 MeV) with a half-life of 1.41×10^{10} years. Manipulations and reactions should be carried out in monitored fume hoods in a radiation laboratory which has α- and β-counting equipment; the laboratory atmosphere is inspected monthly for contamination. Elemental analyses (C, H, and N) were performed by the University of Patras microanalytical service. FT-IR spectra (4000–400 cm^{-1}) were recorded using a PerkinElmer 16PC spectrometer with samples prepared as KBr pellets and as Nujol or hexachlorobutadiene mulls between CsI disks. Solid-state emission and excitation spectra were recorded using a Cary Eclipse fluorescence spectrophotometer. ^{1}H NMR spectra in DMSO-d_6 were recorded using a 400 MHz Bruker Avance DPX spectrometer with TMS as an internal standard. FT-Raman spectra were recorded using a Bruker (D) FRA-106/S component attached to an Equinox 55 spectrometer. An R510 diode-pumped Nd:YAG laser at 1064 nm was used for Raman excitation with a laser power of 250 mW on the sample, utilizing an average of 100 scans at 4 cm^{-1} resolution. Conductivity measurements were carried out at 25 °C with a Metrohm-Herisau E-527 bridge and a cell of standard constant.

Synthetic details

[Th$_4$O(NO$_3$)$_2$(LH)$_2$(L)$_5$]·4MeCN (1·4MeCN). To a colourless solution of Th(NO$_3$)$_4$·5H$_2$O (0.057 g, 0.10 mmol) in MeCN (16 mL) was added solid orange LH$_2$ (0.043 g, 0.20 mmol). The solid soon dissolved and the colour of the solution turned yellow. The reaction solution was stirred for a further 10 min, filtered and stored in a closed flask at room temperature. X-ray quality, yellowish crystals of the product were obtained in a period of 3 d. The crystals were collected by filtration, washed with cold MeCN (2 × 2 mL) and Et$_2$O (3 × 2 mL), and dried *in vacuo* overnight. The yield was ~30% (based on the metal available). The product was analyzed satisfactorily as lattice MeCN-free, *i.e.*, **1**. Analytical data, calcd for C$_{91}$H$_{65}$Th$_4$N$_9$O$_{21}$ (found values are in parentheses): C 42.88 (43.07), H 2.58 (2.52), N 4.95 (4.83)%. IR bands (KBr, cm^{-1}): 3445mb, 3058w, 2924w, 1654w, 1622m, 1604s, 1584m, 1560w, 1542m, 1058w, 1490m, 1472s, 1442w, 1382w, 1314m, 1272m, 1256m, 1172w, 1146w, 1122w, 1032w, 916w, 868w, 834w, 740w, 602w, 484w, 456w, 418w, 404w. Raman peaks (cm^{-1}): 3055wb, ~2700wb, 1625s, 1539s, 1477m, 1437m, 1375m, 1336m, 1266m, 1173m, 1032w, 1010m, 860wb, 766w, 605w, 585w, 579w, 480w, 462w. ^{1}H NMR data (DMSO-d_6, δ/ppm): 13.76 (s), 10.70 (s, br), 10.26 (s), 9.72 (s), 9.38 (s, br), 8.96 (s), 8.91 (d), 8.77 (q), 8.66 (s), 8.61 (d), 8.47 (s, br), 8.18 (t), 7.93 (mt), 7.82 (d), 7.73 (mt), 7.66 (d), 7.60 (d), 7.52 (mt), 7.37 (mt), 7.31 (d), 7.22 (t), 7.12 (t), 7.03 (t), 6.94 (mt), 6.86 (mt), 6.70 (mt), 6.51 (mt), 6.45 (mt), 6.37 (mt), 6.30 (s), 6.16 (mt), 6.03 (mt), 5.87 (mt), 5.79 (d), 5.65 (d), 5.41 (mt), 5.28 (d), 5.17 (d), 5.07 (mt), 4.92 (mt), 4.85 (t), 4.74 (d), 4.08 (q), 2.08 (s). The spectrum refers to a moderately dried sample. Λ_M (DMSO, 10^{-3} M, 25 °C): 86 S cm^2 mol^{-1}.

[Th$_4$O(NO$_3$)$_2$(L′H)$_2$(L′)$_5$]·2.4MeCN (2·2.4MeCN). To a red solution containing L′H$_2$ (0.045 g, 0.20 mmol) in MeCN (16 mL) and Bu$^n_4$NOH (25% solution in MeOH, 57 μL, 0.20 mmol) was added solid Th(NO$_3$)$_4$·5H$_2$O (0.057 g, 0.10 mmol). The solid soon dissolved and the resulting light orange solution was vigorously stirred for 10 min, filtered and stored in a closed flask at room temperature. X-ray quality orange crystals of the product were precipitated over a period of 24 h. The crystals were collected by filtration, washed with cold MeCN (2 mL) and Et$_2$O (3 × 2 mL), and dried *in vacuo* overnight. Typical yields were in the 35–45% range (based on the metal available). The product was analyzed satisfactorily as lattice MeCN-free, *i.e.*, **2**. Analytical data, calcd for C$_{98}$H$_{79}$Th$_4$N$_9$O$_{21}$ (found values are in parentheses): C 44.46 (44.70), H 3.01 (3.11), N 4.76 (4.63)%. IR bands (KBr, cm^{-1}): 3445mb, 3020w, 2918w, 1654w, 1628m, 1602s, 1570w, 1542m, 1498s, 1472s, 1442m, 1384m, 1272m, 1230m, 1196w, 1148w, 1124w, 1030w, 948w, 916w, 858w, 838m, 824w, 756m, 656w, 612w, 550w, 508w, 494w, 458w, 426w, 404m. Raman peaks (cm^{-1}): 3045wb, 2918w, 2860w, 1617m, 1539s, 1500w, 1382m, 1284m, 1235w, 1156w, 1110w, 1039w, 954m, 842w, 761w, 748w, 681w, 595w, 555w, 470wb. ^{1}H NMR data (DMSO-d_6, δ/ppm): 14.08 (d), 13.82 (s), 10.70 (s), 10.26 (s), 9.47 (s), 9.02 (s), 8.96 (s), 8.85 (s), 8.75 (t), 8.28 (mt), 7.91 (mt), 7.52 (mt), 7.35 (mt), 7.17 (d), 6.95 (mt), 6.84 (mt), 6.72 (mt), 6.62 (mt), 6.28 (mt), 5.90 (d), 5.73 (d), 5.55 (d), 4.95 (d), 2.30 (d), 2.23 (s), 2.11 (s), 2.06 (mt), 1.95 (t), 1.75 (d). The spectrum refers to a moderately dried sample. Λ_M (DMSO, 10^{-3} M, 25 °C): 69 S cm^2 mol^{-1}.

Single-crystal X-ray crystallography

Yellowish orange (0.06 × 0.11 × 0.43 mm) and orange (0.17 × 0.17 × 0.36 mm) crystals of **1**·4MeCN and **2**·2.4MecN, respectively, were taken from the mother liquor and immediately cooled to −103 °C (**1**·4MeCN) and −93 °C (**2**·2.4MecN). X-ray diffraction data were collected using a Rigaku R-AXIS SPIDER Image Plate diffractometer using graphite-monochromated Mo Kα radiation. Data collection (ω-scans) and processing (cell refinement, data reduction and empirical absorption correction) were performed using the CrystalClear program package.[61] The structures were solved by direct methods using SHELXS-97 [62] and refined by full-matrix least-squares techniques on F^2 with the latest version of SHELXL (2014/7).[63] The H atoms were either located by difference maps and refined isotropically or were introduced at calculated positions as riding on their respective bonded atoms. All non-H atoms were refined anisotropically. Most structural plots were drawn using the Diamond 3 program package.[64]

Important crystallographic data are listed in Table 1. Full details can be found in the CIF files.

Results and discussion

Synthetic comments

In the present study, we have investigated the reactions between the tridentate Schiff bases LH$_2$ and L′H$_2$ and thorium

 This journal is © The Royal Society of Chemistry 2019

Open Access Article. Published on 02 2019. Downloaded on 2025/7/31 07:35:32.
This article is licensed under a Creative Commons Attribution 3.0 Unported Licence.

Table 1 Crystal data and structure refinement for compounds **1**·4MeCN and **2**·2.4 MeCN

Parameter	**1**·4MeCN	**2**·2.4 MeCN
Formula	$C_{99}H_{77}N_{13}Th_4O_{21}$	$C_{102.8}H_{86.2}N_{11.4}Th_4O_{21}$
F_w	2712.89	2745.39
Crystal system	Triclinic	Monoclinic
Space group	$P\bar{1}$	$P2_1/n$
a/Å	13.5738(3)	16.3097(3)
b/Å	14.9072(3)	26.3838(5)
c/Å	26.8572(5)	22.6412(4)
α/°	81.513(1)	90.0
β/°	76.826(1)	94.057(1)
γ/°	61.585(1)	90.0
V/Å^3	4649.11 (17)	9718.4(3)
Z	2	4
ρ_{calcd}/g cm^{-3}	1.938	1.876
T/K	170	180
Radiation/μ (mm^{-1})	Mo Kα/6.46	Mo Kα/6.18
Reflections collected/ unique (R_{int})	86 266/20 248 (0.049)	91 224/21 120 (0.045)
Reflections with $I > 2\sigma(I)$	16 985	18 560
No. of parameters	1462	1279
$R_1[I > 2\sigma(I)]$, wR_2 (all data)	0.0295, 0.0576	0.0325/0.073
GOF (F^2)	1.02	1.05
$\Delta\rho_{max}/\Delta\rho_{min}$ (e Å^{-3})	1.561/−1.15	2.13/−1.43
CCDC number	1945475	1945476

sources; Th(IV) complexes with these ligands were unknown in the literature. A variety of reaction systems involving $Th(NO_3)_4{\cdot}5H_2O$ and $ThCl_4$, solvent media, reaction ratios, the absence/presence of external bases and crystallization techniques were systematically studied for arriving at the optimized procedures described in the Experimental section. Working with $ThCl_4$, we obtained powders which could not be crystallized; IR spectroscopy indicated that the powders were products.

Treatment of $Th(NO_3)_4{\cdot}5H_2O$ and LH_2 (1 : 2) in MeCN at room temperature gave a yellow solution from which were subsequently isolated yellowish crystal of $[Th_4O(NO_3)_2(LH)_2(L)_5]{\cdot}$4MeCN (**1**·4MeCN) in rather low yields (~30%), eqn (1). Efforts to prepare a compound with all the ligands in their doubly deprotonated form (L^{2-}), *e.g.*, $[Th_4O(L)_7]$ were not successful, even when we used an external base (Et_3N, $Bu^n{}_4NOH$) to LH_2 ratios up to 2 : 1. The obtained product was again **1**; somewhat to our surprise the yield of the reaction increased only by 10%, reaching 40–45% (the procedure with the addition of the base is not described in the Experimental section).

$$4Th(NO_3)\cdot 5H_2O + 7LH_2 \xrightarrow{MeCN} [Th_4O(NO_3)_2(LH_2)(L)_5] + 14HNO_3 + 19H_2O \quad (1)$$

A completely analogous reaction between $Th(NO_3)_4{\cdot}5H_2O$ and $L'H_2$ in MeCN, using the same concentrations of the reactants as in the case of **1**, resulted only in a few orange crystals (yield lower than 10%) of $[Th_4O(NO_3)_2(L'H)_2(L')_5]{\cdot}$2.4MeCN (**2**·2.4MeCN). The addition of an external base was deemed necessary to increase the yield. Thus, the $Th(NO_3)_4{\cdot}5H_2O/L'H_2/Bu^n{}_4NOH$ (1 : 2 : 2) reaction system in MeCN gave a light orange solution, from which the product was isolated in a *ca.* 40% yield, eqn (2). Increase of the $L'H_2$ to OH^- ratio from 2 : 2 to 2 : 4, to further improve the yield, resulted in the precipitate of amorphous hydroxide thorium(IV) species.

$$4Th(NO_3)\cdot 5H_2O + 7L'H_2 + 7Bu^n_4NOH \xrightarrow{MeCN} [Th_4O(NO_3)_2(L'H_2)(L')_5] + 14(Bu^n_4N)NO_3 + 7HNO_3 + 26H_2O \quad (2)$$

Description of the structures

Aspects of the molecular and crystal structures of complexes **1**·4MeCN and **2**·2.4MeCN are shown in Fig. 1–6 and Fig S1–S3.‡ Selected numerical data are listed in Tables 2, 3 and S1–S5.‡ The molecular structures of the two complexes are very similar. Thus, only the molecular structure of **1**·4MeCN will be described in detail.

The crystal structure of **1**·4MeCN consists of molecules $[Th_4O(NO_3)_2(LH)_2(L)_5]$ and MeCN in an 1 : 4 ratio. The tetranuclear molecule (Fig. 1) contains four Th^{IV} atoms arranged at

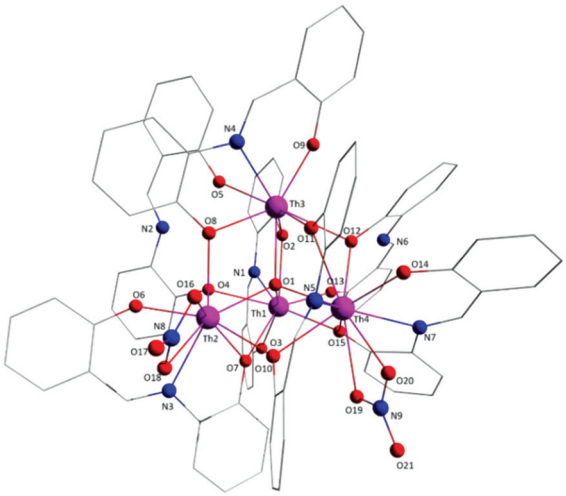

Fig. 1 Partially labelled plot of the tetranuclear molecule that is present in the structure of **1**·4MeCN. Colour scheme: Th, pink; O, red; N, blue; C, grey. All H atoms have been omitted for clarity.

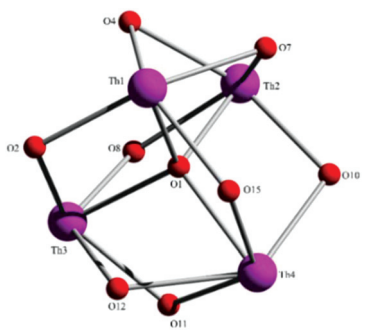

Fig. 2 The $\{Th^{IV}_4(\mu_4\text{-}O)(\mu\text{-}OR')_8\}$ core of molecules **1** and **2**. O1 is the μ_4-O^{2-} group in **1**, O4 and O12 are the bridging oxygen atoms of the iminiumphenolate parts of the LH^- in **1** ligands, while the remaining oxygen atoms belong to the L^{2-} groups.

Open Access Article. Published on 02 2019. Downloaded on 2025/7/31 07:35:32.
This article is licensed under a Creative Commons Attribution 3.0 Unported Licence.

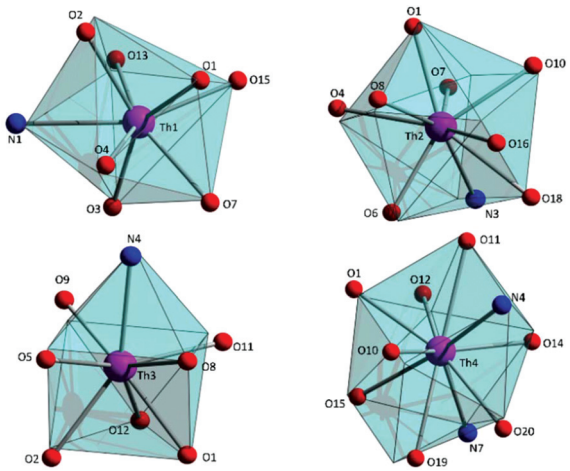

Fig. 3 The triangular dodecahedral, muffin-type, biaugmented trigonal prismatic and sphenocorona coordination polyhedra for Th1, Th2, Th3 and Th4, respectively, in the structure of **1**·4MeCN. The very small spheres define the vertices of the ideal polyhedra.

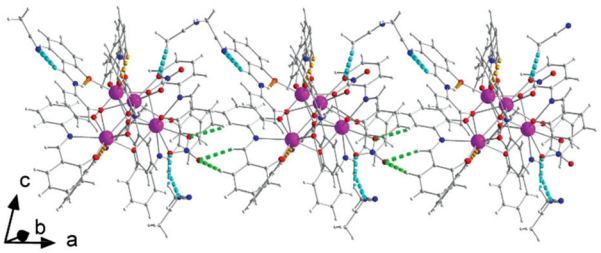

Fig. 4 A portion of a chain of tetranuclear cluster and MeCN molecules parallel to the α crystallographic axis in the crystal structure of **1**·4MeCN. Dashed orange lines indicate intramolecular N–H···O bonds within the LH^- ligands and dashed cyan lines indicate H bonds involving the lattice MeCN molecules; dashed light green lines represent the H bonds that are responsible for the formation of chains.

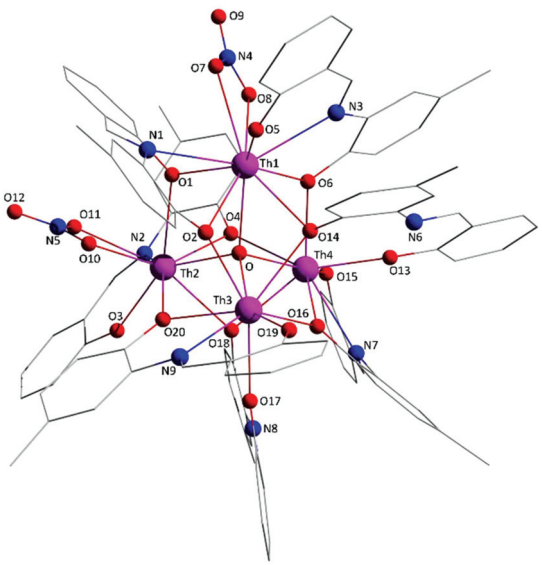

Fig. 5 Partially labelled plot of the tetranuclear molecule that is present in the structure of **2**·2.4MeCN. Colour scheme: Th, pink; O, red; N, blue; C, grey. All H atoms have been omitted for clarity.

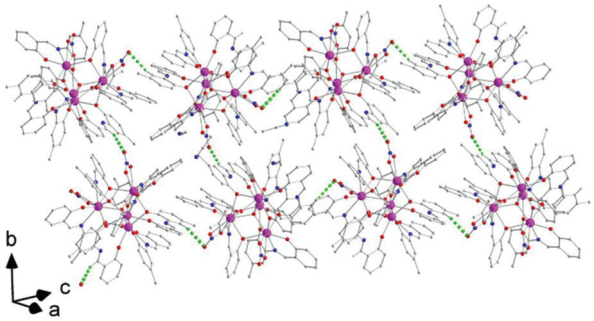

Fig. 6 A part of a layer parallel to the (–101) plane formed as a result of C–H···O H bonds (dashed light green lines) between the tetranuclear cluster molecules in the crystal structure of **2**·2.4MeCN, see the text for details. Only the H atoms involved in H bonds that contribute to the layer formation are shown.

Table 2 Selected interatomic distances (Å) and angles (°) for complex **1**·4MeCN

Distances			
Th1···Th2	3.776(1)	Th2···Th3	3.992(1)
Th1···Th3	3.935(1)	Th2···Th4	4.001(1)
Th1···Th4	4.039(1)	Th3···Th4	3.816(1)
Th1–O1	2.434(3)	Th3–O2	2.447(3)
Th1–O2	2.410(3)	Th3–O5	2.372(3)
Th1–O3	2.205(3)	Th3–O8	2.436(3)
Th1–O4	2.486(3)	Th3–O9	2.228(3)
Th1–O7	2.463(3)	Th3–O11	2.379(3)
Th1–O13	2.335(3)	Th3–O12	2.574(3)
Th1–O15	2.437(3)	Th3–N4	2.601(4)
Th1–N1	2.650(3)	Th4–O1	2.440(3)
Th2–O1	2.369(3)	Th4–O10	2.493(4)
Th2–O4	2.566(3)	Th4–O11	2.598(3)
Th2–O6	2.235(3)	Th4–O12	2.579(3)
Th2–O7	2.459(3)	Th4–O14	2.213(3)
Th2–O8	2.511(3)	Th4–O15	2.479(3)
Th2–O10	2.445(3)	Th4–O19	2.652(3)
Th2–O16	2.573(3)	Th4–O20	2.574(3)
Th2–O18	2.612(3)	Th4–N5	2.741(4)
Th2–N3	2.636(4)	Th4–N7	2.660(4)
Th3–O1	2.380(3)		
Angles			
Th1–O1–Th2	103.7(1)	Th2–O1–Th3	114.4(1)
Th1–O1–Th3	109.7(1)	Th2–O1–Th4	112.6(1)
Th1–O1–Th4	111.9(1)	Th3–O1–Th4	104.7(1)
O4–Th1–O13	148.7(1)	Th1–O7–Th2	100.2(1)
O6–Th2–O10	153.6(1)	Th2–O8–Th3	107.6(1)
O1–Th3–O9	150.3(1)	Th3–O11–Th4	100.0(1)
O11–Th4–O19	161.2(1)	Th1–O15–Th4	110.5(1)

the vertexes of a distorted tetrahedron, with a central μ_4-O^{2-} ion (O1) bonded to each metal ion. The Th^{IV} centres are also held together by two 3.21 (Harris notation[65]) LH^- groups, one 3.221 L^{2-} and four 2.211 L^{2-} ligands (Scheme 2). Two slightly anisobidentate chelating nitrato groups (donor atoms O16/O18 and O19/O20) complete the coordination spheres of Th2 and Th4. The core of the molecule is $\{Th^{IV}_4(\mu_4\text{-}O)(\mu\text{-}OR')_8\}$ (Fig. 2). Of interest is the fact that the H atom of one of the acidic –OH groups of each LH^- ligand is clearly located on the imine nitrogen atom (N2 and N6), thus blocking the coordination of the latter.

This journal is © The Royal Society of Chemistry 2019

Open Access Article. Published on 02 2019. Downloaded on 2025/7/31 07:35:32.
This article is licensed under a Creative Commons Attribution 3.0 Unported Licence.

Table 3 Selected interatomic distances (Å) and angles (°) for complex **2**·2.4 MeCN

Distances			
Th1···Th2	4.029(1)	Th2···Th3	3.988(1)
Th1···Th3	3.823(1)	Th2···Th4	3.763(1)
Th1···Th4	4.029(1)	Th3···Th4	3.942(1)
Th1–O	2.438(3)	Th2–N2	2.633(4)
Th1–O1	2.483(3)	Th3–O	2.379(3)
Th1–O2	2.660(3)	Th3–O2	2.379(3)
Th1–O5	2.195(3)	Th3–O14	2.539(3)
Th1–O6	2.467(3)	Th3–O16	2.435(3)
Th1–O7	2.642(3)	Th3–O17	2.386(3)
Th1–O8	2.642(3)	Th3–O19	2.241(3)
Th1–O14	2.585(3)	Th3–O20	2.413(3)
Th1–N1	2.725(4)	Th3–N9	2.618(4)
Th1–N3	2.693(3)	Th4–O	2.427(3)
Th2–O	2.384(3)	Th4–O4	2.440(3)
Th2–O1	2.504(3)	Th4–O6	2.421(3)
Th2–O3	2.230(3)	Th4–O13	2.321(3)
Th2–O4	2.462(3)	Th4–O15	2.235(3)
Th2–O10	2.561(3)	Th4–O16	2.406(3)
Th2–O11	2.621(3)	Th4–O18	2.534(3)
Th2–O18	2.497(3)	Th4–N7	2.644(4)
Th2–O20	2.529(3)		
Angles			
Th1–O–Th2	113.3(1)	Th2–O–Th3	113.7(1)
Th1–O–Th3	105.1(1)	Th2–O–Th4	102.9(1)
Th1–O–Th4	111.8(1)	Th3–O–Th4	110.2(1)
O6–Th1–N1	156.5(1)	Th1–O1–Th2	107.8(1)
O20–Th2–N2	154.0(1)	Th2–O4–Th4	100.3(1)
O2–Th3–O17	151.9(1)	Th1–O14–Th3	96.5(1)
O–Th4–O15	148.0(1)	Th2–O18–Th4	96.8(1)

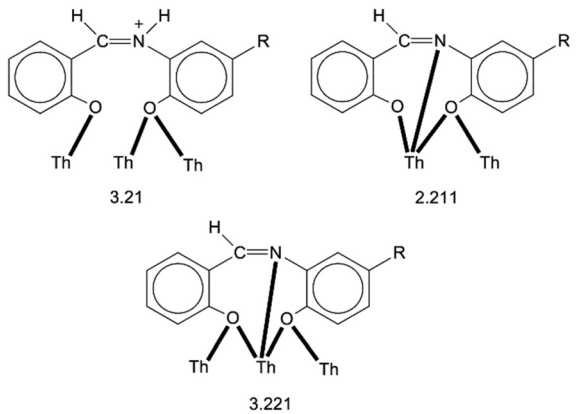

Scheme 2 The crystallographically established coordination modes of LH^- (R = H), L^{2-} (R = H), $L'H^-$ (R = Me) and $(L')^{2-}$ (R = Me) in complexes **1**·4MeCN and **2**·2.4MeCN, and the Harris notation that describes these modes.

The $Th^{IV}\cdots Th^{IV}$ separations range from 3.776(1) to 4.039(1) Å. The Th1···Th2 [3.776(1) Å] and Th3···Th4 [3.816(1) Å] distances are shorter than the other four $Th^{IV}\cdots Th^{IV}$ distances [3.935(1)–4.039(1) Å], because the Th1/Th2 and Th3/Th4 pairs are linked by three monoatomic O bridges (O1, O4, and O7 for the Th1/Th2 pair; O1, O11, and O12 for the Th3/Th4 pairs), whereas the Th1/Th3, Th1/Th4, Th2/Th3 and Th2/Th4 pairs are each connected by two monoatomic O bridges (O1 and one phenoxido O atom). The Th^{IV}–(μ_4-O^{2-})–Th^{IV} angles are in the 103.7(1)–112.6(1)° range, in agreement with the distorted tetrahedral arrangement of the metal centres. Th1 is 8 coordinate; it is coordinated by seven oxygen atoms, with the Th1–O bond lengths ranging from 2.205(3) to 2.486(3) Å and one nitrogen atom. Two oxygen atoms are terminal from one LH^- (O13) and one L^{2-} (O3) ligands, four are bridging from a LH^- (O4) and three L^{2-} (O2, O7, and O15) ligands and the seventh oxygen atom is the oxido group. Th2 is 9-coordinate; it is surrounded by eight oxygen atoms, with the Th2–O bond lengths ranging from 2.235(3) to 2.612(3) Å, and by one nitrogen atom. One oxygen atom is bridging from a LH^- (O4) ligand, four oxygen atoms (one terminal, O6; three bridging, O7/O8/O10) belong to three L^{2-} ligands, two oxygen atoms are from a chelating nitrato group (O16 and O18) and the eighth oxygen is the oxido group. Th3 is 8-coordinate; it is bonded to seven oxygen atoms, with the Th3–O bond length ranging from 2.228(3) to 2.574(3) Å, and to one nitrogen atom. Two oxygen atoms are terminal from one LH^- (O5) and one L^{2-} (O9) ligands, four are bridging from a LH^- (O12) and three L^{2-} (O2, O8, and O11) ligands and the seventh oxygen atom is the oxido group. Finally, Th4 is surrounded by eight oxygen and two nitrogen atoms being 10-coordinate. The Th4–O bond lengths range from 2.213(3) to 2.652(3) Å. One oxygen atom is bridging from a LH^- (O12) ligand, four oxygen atoms (one terminal, O14; three bridging, O10/O11/O15) belong to two L^{2-} ligands, two oxygen atoms are from a chelating nitrato group (O19 and O20) and the eighth oxygen atom is the oxido group. The Th–N bond distances are in the range of 2.601(4)–2.741(4) Å and are typical for 8-, 9- and 10-coordinate species with Schiff bases as ligands.[40–45]

To estimate the closer coordination polyhedra defined by the donor atoms around the Th^{IV} centres in **1**·4MeCN, a comparison of the experimental structural data with the theoretical values for the most common polyhedral shapes with 8, 9 and 10 vertices was performed using the SHAPE program.[66] The best fit was obtained for the triangular dodecahedron (Th1), the muffin (Th2), the biaugmented trigonal prism (Th3) and sphenocorona (Th4) (Fig. 3 and Tables S3–S5‡).

There are two classical, relatively strong, intraligand H bonds within the tetranuclear molecule (Fig. S1, Table S1‡), with the protonated nitrogen atoms (N2 and N6) of the LH^- ligands as donors and their terminal, formerly salicylaldehyde, phenolato oxygen atoms (O5 and O13) as acceptors. A variety of intermolecular H-bonding interactions are present in the crystal structure. Three lattice MeCN molecules, three coordinated nitrato oxygen atoms (O16, O19, and O20) and one non-coordinated nitrato oxygen atom (O21) act as acceptors, while the donors are aromatic and aliphatic carbon atoms from the ligands and MeCN. The overall result is the formation of chains parallel to the α axis (Fig. 4).

Molecule **2** has a very similar structure (Fig. 5 and S2‡) to that of **1** (Fig. 1). The core, the metal topology, the coordination polyhedra (Fig. S3, Tables S3–S5‡) and the coordination modes of the organic and nitrato ligands are almost identical in the two structures. In the numbering schemes of the metal centres, Th1, Th2, Th3 and Th4 in **2** are equivalent to Th4,

Open Access Article. Published on 02 2019. Downloaded on 2025/7/31 07:35:32.
This article is licensed under a Creative Commons Attribution 3.0 Unported Licence.

Th2, Th3 and Th1, respectively, in **1**. The $Th^{IV}\cdots Th^{IV}$ distances and the Th^{IV}–(μ_4-O^{2-})–Th^{IV} angles are in the ranges 3.763(1)–4.029(1) Å [3.776(1)–4.039(1) Å in **1**·4MeCN] and 102.9(1)–113.7(1)° [103.7(1)–112.6(1)° in **1**·4MeCN], respectively. At the supramolecular level, the tetranuclear $[Th_4O(NO_3)_2(L'H)_2(L')_5]$ molecules are connected through H bonds forming layers parallel to the (−101) plane (Fig. 6). The acceptors are the non-coordinated oxygen atoms O9 and O12 of the nitrato groups, and the donors are the imine carbon atom one $L'H^-$ ligand and one aromatic carbon atom of the iminium phenolato part of the other $L'H^-$ ligand.

Complexes **1**·4MeCN and **2**·2.4MeCN are the third and fourth, respectively, tetranuclear thorium(IV) complexes with the tetrahedral $\{Th^{IV}_4(\mu_4\text{-}O)\}$ unit. The previously structurally characterized examples are complexes $[Th_4OCl_8(EO4)_3]$,[67] where EO4 is the tetraethylene glycolate(−2) ligand, and $[Th_4OCl_2I_6\{O(CH_2)_2OCH_3\}_6]$.[68] Interestingly, the authors note that the oxido bridge in the former complex is the result of an oxide impurity from the $ThCl_4$ starting material.[67] In the latter complex, the source of the central μ_4-O^{2-} unit was verified to be[68] dimethoxyethane (DME) present in the starting $[Th_4Cl_{4-x}I_x(DME)_2]$ material, and not adventitious H_2O (the reaction and the manipulation were performed in a strictly inert atmosphere (N_2) under vacuum). In the case of **1** and **2**, the source of the oxido group seems to be H_2O from the solvent (MeCN) and the hydrated thorium(IV) nitrate. Such μ_4-O^{2-} groups are extremely rare in An(IV) cluster chemistry despite their occurrence in the fluorite-type structures.[8] Generally, the tetravalent actinides Th–Pu represent some of the hardest cations of the Periodic table; because of their high charge density and acidity, these metal ions are particularly prone to hydrolysis and condensation.[9,18]

Compounds **1** and **2** are new members of a large family of complexes of 3d-, 4f- and mixed 3d/4f-metal ions (ref. 47–54 are only representative) containing anionic forms of LH_2 and $L'H_2$. However, they join a handful of structurally characterized An complexes which are listed in Table 4. Unfortunately, no U(IV), Np(IV) and Pu(IV) complexes with any forms of LH_2 and $L'H_2$ have been reported, so no direct comparison of An complexes with the metal in the IV oxidation state are possible. The previous An examples were mononuclear (neutral[69] and anionic[34,70]) and dinuclear[55] uranyl (UO_2^{2+}) complexes. The completely different structures between the uranyl and thorium(IV) complexes (Table 4) are attributed to the completely different chemical nature of the two metal species. In a general sense, as compared to the hexavalent actinides, which almost invariably form the well-established actinyl cation ($An^{VI}O_2^{2+}$), the tetravalent actinides adopt more spherical or isotropic coordination geometries, thus leading to structural units and types that are quite distinct from those of the hexavalent An ions.[18] Restricting this discussion to Th(IV) and $U^{VI}O_2^{2+}$, Th(IV) exhibits an effective charge that matches its formal oxidation state, whereas U(VI), in the form of the uranyl species, behaves as a metal ion with an effective charge of +3.3.[10]

A final interesting point is the fact that the 3.210 ligation mode of LH^- and $L'H^-$ established in the structures of **1**·4MeCN and **2**·2.4MeCN, respectively, is observed for the first time in the coordination chemistry of LH_2 and $L'H_2$.

Table 4 To-date structurally characterized 5f-element complexes of the anionic forms of LH_2 and $L'H_2$

Complex[a]	Coordination mode of the ligand	Ref.
$[UO_2(L)_2(DMSO)_2]$	1.111	69
$(Bu^n_4N)_2[UO_2(L)(H_2PO_4)_2]$	1.111	70
$[(UO_2)_2(L')_2(E\tau OH)_2]^b$	2.211	55
$[Th_4O(NO_3)_2(LH)_2(L)_5]$	3.21,[c] 2.211,[d] 3.221[d]	This work
$[Th_4O(NO_3)_2(L'H)_2(L')_5]$	3.21,[c] 2.211,[d] 3.221[d]	

[a] The lattice solvent molecules have been omitted. [b] A similar complex $[(UO_2)_2(L'')_2(EtOH)_2]$, where $(L'')^{2-}$ is the dianion of *N*-salicylidene-*o*-amino-4-chlorophenol ($L''H_2$; R = Cl in Scheme 1), has also been structurally characterized.[55] [c] For the monoanionic ligands. [d] For the dianionic ligands.

Spectroscopic studies

In the IR spectra of **1** and **2** (Fig. S4 and S5‡), the medium-intensity and broad band at ~3450 cm^{-1} is attributed to the $\nu(NH^+)$ vibration of the LH^- or $L'H^-$ ligands (*vide supra*);[71] the broadness of the band is indicative of H bonding. The spectrum of **1** exhibits a medium-intensity and a strong band at 1622 and 1604 cm^{-1}, respectively, which is assigned[46,55,71] to the C=N stretching vibration, ν(C=N), of the Schiff base linkage. These bands have been shifted to lower wavenumbers compared with the corresponding band in the spectrum of the free LH_2 ligand (1630 cm^{-1}, Fig. S6‡), in agreement with the protonation or coordination of the imine nitrogen. The appearance of the two bands reflects the presence of two types (protonated and coordinated) of C=N groups in the complex. The two bands appear at 1628 and 1602 cm^{-1} in the spectrum of **2**. The band at 1602 cm^{-1} has been shifted to a lower wavenumber compared with the band in the spectrum of the free $L'H_2$ ligand (1628 cm^{-1}, Fig. S7‡), whereas the band at 1628 cm^{-1} has remained at the same wavenumber. The latter experimental fact is not unusual.[72,73] Extensive experimental and theoretical studies on complexes with Schiff bases containing a C=N bond (with the carbon atom attached to an aromatic ring) have revealed that a change in the s character of the N lone pair occurs upon coordination or protonation and the s character of the N orbital involved in the C=N bond increases; this change in hybridization leads to a greater C=N stretching constant relative to the free neutral ligands, thus shifting the ν(C=N) vibrational mode to slightly higher wavenumbers. The IR bands at ~1470, ~1270 and ~1030 cm^{-1} in the spectra of both complexes are assigned[74] to the $\nu_1(A_1)[\nu(N{=}O)]$, $\nu_5(B_2)[\nu_{as}(NO_2)]$ and $\nu_2(A_1)[\nu_s(NO_2)]$ vibrations of the bidentate chelating (C_{2v}) nitrato group; the separation of the two highest-wavenumber stretching bands is ~200 cm^{-1}, in agreement with the bidentate character of the coordinated nitrato groups.[52,74]

The Raman spectra of the well dried samples of complexes **2** and **1** are shown in Fig. 7 and S8,‡ respectively. The characteristic $\nu(C_{aromatic}\text{–}H)$ peak appears at ~3050 cm^{-1} in both

 This journal is © The Royal Society of Chemistry 2019

Open Access Article. Published on 02 2019. Downloaded on 2025/7/31 07:35:32.
This article is licensed under a Creative Commons Attribution 3.0 Unported Licence.

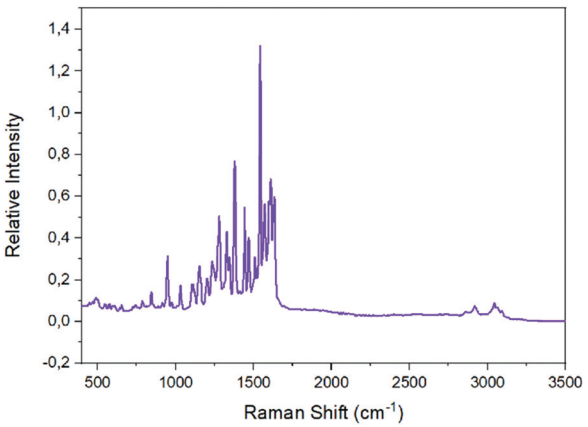

Fig. 7 The Raman spectrum of **2**.

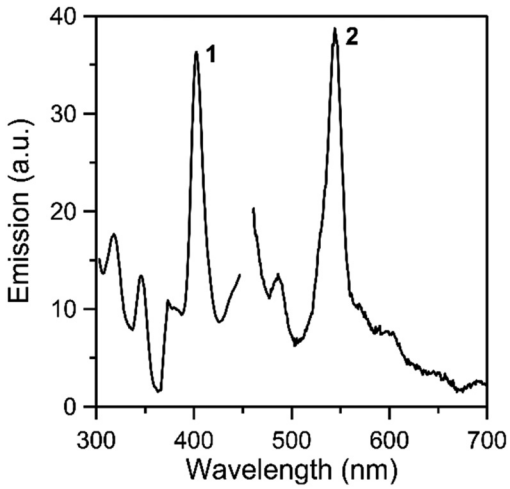

Fig. 8 Solid-state, room-temperature excitation (curve 1; maximum emission at 540 nm) and emission (curve 2; maximum excitation at 400 nm) spectra of complex **1**.

spectra;[11,46,72,75,76] extra peaks at 2918 and 2860 cm^{-1} in the spectrum of **2** are due to the $\nu_{as}(CH_3)$ and $\nu_s(CH_3)$ modes, respectively.[46,75] The peak at ~1620 cm^{-1} in both spectra is due to the ν(C=N) mode of the Schiff-base linkage;[46,76] the clear splitting of this peak reflects the presence of two types of imine linkages (protonated and coordinated) in the tetranuclear complexes. The two highest-frequency stretching nitrogen–oxygen vibrations of the bidentate chelating nitrato groups are located[74,77] at 1477 and 1266 cm^{-1} for **1**, and at 1500 and 1284 cm^{-1} for **2**.

The ^{1}H NMR spectra of **1** and **2** in DMSO-d_6 (Fig. S9 and S10‡) are extremely complicated, suggesting the presence of several different species in solution and indicating that the structures of the complexes are not retained in solution. For example, the spectrum of **2** shows four signals between δ 2.00 and 2.30 ppm, with different integration ratios, attributed[11,46] to the protons of the methyl groups. The imine protons appear around δ 9 ppm in the form of multiple signals.[43] Of particular interest is the appearance of signals at δ values in the region 14.08–13.76 ppm and at ~9.7 ppm. The former can be assigned to the very acidic protons of –C=NH^+ groups from the LH^- and $L'H^-$ ligands; the latter most probably indicates the presence of –OH groups arising from protonation of the deprotonated phenolato oxygen atoms, the most possible proton sources being some of the –C=NH^+ groups and/or hydrolysis of $[Th(H_2O)_x]^{4+}$ species; a strong evidence of hydrolytic processes comes from the appearance of signals in the δ 4.8–6.2 ppm region assigned[11] to coordinated OH^- groups. Our proposal for the decomposition of the complexes in solution is reinforced by the molar conductivity values, Λ_M (10^{-3} M, 25 °C), in DMSO, which are 86 (**1**) and 69 (**2**) S cm^2 mol^{-1}; these values indicate the presence of ionic species in this solvent.[78]

Solid-state, room-temperature emission spectra of the free ligands LH_2 and $L'H_2$ (Fig. S11 and S12,‡ respectively), and complexes **1** and **2** (Fig. 8 and S13‡) were recorded. The optical behavior of the two complexes is similar. Upon maximum excitation at 400 nm, the solid complexes show a rather sharp emission band with a maximum at ~ 540 nm (emission of green light). As Th(IV) is non-emissive, the emission can be assigned to a charge transfer state within the coordinated organic ligands.[44,79–84] Tetravalent thorium has a $5f^0$ configuration. All of the electrons are spin paired in this electronic state and emission is not expected.[81] It is also hardly oxidizing and consequently low-energy metal-centered charge-transfer excited states do not exist.[80] Additional evidence for the intraligand character of the green emission in the complexes comes from the study of the emission properties of the free ligands. Upon maximum excitation at 497 nm (LH_2) or 465 nm ($L'H_2$), the ligands emit at 540 nm (LH_2) and 610 nm ($L'H_2$). The development of "turn-on" or "turn-off" fluorescent sensors for Th(IV) is an area of intense interest due to their potential use for thorium analysis/identification in nuclear waste investigation.[44,82–84]

Conclusions and perspectives

Even at the time of submission of the present work, thorium chemistry continues to surprise the inorganic chemistry community.[85–91] For example, the number of the crystallographically characterised Th(III) complexes (mainly with cyclopentadienyl ancillary ligands) increases and the first example of a square planar thorium complex has been just reported.[89] Many scientists believe that with the harmful effects of global climate change becoming more evident with every passing year, more research activity and allocated resources will help the Z = 90 element realize its great potential and become a truly valuable source of materials in our energy economy.[5]

As far as the present work is concerned, it is rather difficult to conclude on a research topic, *i.e.*, Th(IV) complexes with Schiff-base ligands, which is still at its infancy. In this report, we believe that we have contributed to some extent into the chemistry of thorium(IV) clusters, and into the coordination chemistry of LH_2 and $L'H_2$ and related tridentate Schiff bases.

Open Access Article. Published on 02 2019. Downloaded on 2025/7/31 07:35:32.
This article is licensed under a Creative Commons Attribution 3.0 Unported Licence.

Complexes **1** and **2** have interesting molecular structures and contain the extremely rare $\{Th^{IV}_4(\mu_4\text{-}O)\}^{14+}$ core. They also join a handful of fluorescent Th(IV) complexes. The observed ligand-based green emission might indicate that LH_2 and $L'H_2$ and related tridentate Schiff bases containing naptholate (instead of phenolate) aromatic rings, can be considered to be fluorescent sensors for toxic Th(IV) analysis. The development of such a fluorescence detection in solution might provide a simple, rapid, selective and low-cost method for thorium ion determination. Several fluorogenic optodes for Th(IV), with a variety of organic molecules as sensing materials, have been developed in the last 10 years or so. However, some limitations such as a poor sensitivity, a limited working pH range and minor or major interference from other metal ions (*e.g.* Al^{3+}, UO_2^{2+}, Ti^{4+}, Zr^{4+} and trivalent lanthanides), due to their similar chemical properties, need to be addressed. Very recently Kumar and Kumar designed, synthesized, fabricated and used an excellent 8-aminoquinoline-based fluorescent optode for the quantification of Th^{4+} in various aqueous, monazite sand and gas mantle samples.[92] In the present case, the ligand $L'H_2$ could be, in principle, used as the sensor of Th(IV) in the presence of UO_2^{2+}, since the complex of the latter with $(L')^{2-}$ does not emit light at room temperature under several excitation wavelengths.[55]

Future work will be focused on the study of the coordination chemistry of tetradentate Schiff bases containing one –OH and one –COOH group (instead of two –OH groups) on different aromatic rings towards Th(IV) and the investigation of the emission properties of Th(IV) complexes in solution. Work is also in progress to develop the Th(IV)-oxime/oximate chemistry (oximes also contain a C=N group) and synthesize the almost elusive thorium η^2-(O,N)-oximate complexes.[93] These efforts, already well advanced, will be reported in due course.

Conflicts of interest

There are no conflicts to declare.

Acknowledgements

We thank the Research Director George Voyiatzis (ICE-HT/FORTH) for helpful discussion concerning the Raman spectra of the complexes and Dr Zoi G. Lada for recording these spectra.

Notes and references

1 N. R. Andreychuk, T. Dickie, D. J. H. Emslie and H. A. Jenkins, *Dalton Trans.*, 2018, **47**, 4866–4876.
2 F. A. Cotton, G. Wilkinson, C. A. Murillo and M. Bochmann, *Advanced Inorganic Chemistry*, Wiley, New York, 6th edn, 1999, pp. 1130–1164.
3 C. E. Housecroft and A. G. Sharpe, *Inorganic Chemistry*, Pearson Harlow, UK, 5th edn, 2018, pp. 1033–1064.
4 M. S. Wickleder, B. Fourest and P. K. Dorhout, in *The Chemistry of the Actinide and Transactinide Elements*, ed. L. R. Morss, N. M. Edelstein and J. Fuger, Springer, Dordrecht, The Netherlands, 4th edn, 2010, vol. 1, ch. 3, pp. 52–133.
5 J. Arnold, T. L. Gianetti and Y. Kashtan, *Nat. Chem.*, 2014, **6**, 554.
6 L. S. Natrajan, A. N. Swinburne, M. B. Andrews, S. Randall and S. L. Heath, *Coord. Chem. Rev.*, 2014, **266–267**, 171–193.
7 C. D. Tutson and A. E. V. Gorden, *Coord. Chem. Rev.*, 2017, **333**, 27–43.
8 J. Qiu and P. C. Burns, *Chem. Rev.*, 2013, **113**, 1097–1120.
9 K. E. Knope and L. Soderholm, *Chem. Rev.*, 2013, **113**, 944–994.
10 P. O. Adelani and T. E. Albrecht-Schmitt, *Inorg. Chem.*, 2010, **49**, 5701–5705.
11 M. Vasiliu, K. E. Knope, L. Soderholm and D. A. Dixon, *J. Phys. Chem. A*, 2012, **116**, 6917–6926.
12 E. P. Wildman, G. Balázs, A. J. Wooles, M. Scheer and S. T. Liddle, *Nat. Commun.*, 2016, **7**, 12884.
13 P. K. Mohapatra, *Dalton Trans.*, 2017, **46**, 1730–1747 (perspective).
14 S. S. Galley, C. E. Van Alstine, L. Maron and T. E. Albrecht-Schmitt, *Inorg. Chem.*, 2017, **56**, 12692–12694.
15 C. Falaise, K. Kozma and M. Nyman, *Chem. – Eur. J.*, 2018, **24**, 14226–14232.
16 Z. Wang, A. T. Brown, K. Tan, Y. J. Chabal and K. J. Balkus Jr., *J. Am. Chem. Soc.*, 2018, **140**, 14735–14739.
17 A. McSkimming, J. Su, T. Cheisson, M. R. Gau, P. J. Carroll, E. R. Batista, P. Yang and E. J. Schelter, *Inorg. Chem.*, 2018, **57**, 4387–4394.
18 N. A. Vanagas, J. N. Wacker, C. L. Rom, E. N. Glass, I. Colliard, Y. Qiao, J. A. Bertke, E. Van Keuren, E. J. Schelter, M. Nyman and K. E. Knope, *Inorg. Chem.*, 2018, **57**, 7259–7269.
19 P. Li, S. Goswami, K.-i. Otake, X. Wang, Z. Chen, S. L. Hanna and O. K. Farha, *Inorg. Chem.*, 2019, **58**, 3586–3590.
20 O. A. Ejegbavwo, C. R. Martin, O. A. Olorunfemi, G. A. Leith, R. T. Ly, A. M. Rice, E. A. Dolgopolova, M. D. Smith, S. G. Karakalos, N. Birkner, B. A. Powell, S. Pandey, R. J. Koch, S. T. Misture, H.-C. zur Loye, S. R. Phillpot, K. S. Brinkman and N. B. Shustova, *J. Am. Chem. Soc.*, 2019, **141**, 11628–11640.
21 M. Nakase, T. Yamamura, K. Shirasaki, M. Nagai and K. Takeshita, *Sep. Sci. Technol.*, 2019, **54**, 1952–1959.
22 M. Lung and O. Gremm, *Nucl. Eng. Des.*, 1998, **180**, 133–146.
23 M. Follows, Educ. Chem., Is thorium the perfect fuel? | Feature | Education in Chemistry, https://eic.rsc.org/feature/is-thorium-the-perfect-fuel/2000092.article, (accessed 26 July 2019).
24 Y. Dong, S. Li, X. Su, Y. Wang, Y. Shen and X. Sun, *Hydrometallurgy*, 2017, **171**, 387–393.
25 Z. Zhu, Y. Pranolo and C. Y. Cheng, *Miner. Eng.*, 2015, **77**, 185–196.

 This journal is © The Royal Society of Chemistry 2019

Open Access Article. Published on 02 2019. Downloaded on 2025/7/31 07:35:32.
This article is licensed under a Creative Commons Attribution 3.0 Unported Licence.

26 L. Salmon, P. Thuéry, E. Rivière and M. Ephritikhine, *Inorg. Chem.*, 2006, **45**, 83–93.
27 T. Tidwell, *Angew. Chem., Int. Ed.*, 2008, **47**, 1016–1020.
28 J. Costamagna, J. Vargas, R. Latorre, A. Alvarado and G. Mena, *Coord. Chem. Rev.*, 1992, **119**, 67–88.
29 S. Yamada, *Coord. Chem. Rev.*, 1999, **190–192**, 537–555.
30 P. G. Cozzi, *Chem. Soc. Rev.*, 2004, **33**, 410–421.
31 K. C. Gupta and A. K. Sutar, *Coord. Chem. Rev.*, 2008, **252**, 1420–1450.
32 M. E. Belowich and J. F. Stoddart, *Chem. Soc. Rev.*, 2012, **41**, 2003–2024.
33 C. D. Meyer, C. S. Joiner and J. F. Stoddart, *Chem. Soc. Rev.*, 2007, **36**, 1705–1723.
34 D. M. Rudkevich, W. Verboom, Z. Brzozka, M. J. Palys, W. P. R. V. Stauthamer, G. J. van Hummel, S. M. Franken, S. Harkema, J. F. J. Engbersen and D. N. Reinhoudt, *J. Am. Chem. Soc.*, 1994, **116**, 4341–4351.
35 J. L. Sessler, T. D. Mody and V. Lynch, *Inorg. Chem.*, 1992, **31**, 529–531.
36 P. L. Arnold, A. J. Blake, C. Wilson and J. B. Love, *Inorg. Chem.*, 2004, **43**, 8206–8208.
37 M. S. Bharara, S. A. Tonks and A. E. V. Gorden, *Chem. Commun.*, 2007, 4006–4008.
38 K. Takao, M. Kato, S. Takao, A. Nagasawa, G. Bernhard, C. Hennig and Y. Ikeda, *Inorg. Chem.*, 2010, **49**, 2349–2359.
39 C. A. Hawkins, C. G. Bustillos, R. Copping, I. May and M. Nilsson, *Actinide and Fission Product Partitioning and Transmutation*, NEA/NSC/R, 2015, vol. 2, pp. 315–323.
40 For example, see: A. Bino and R. Chayat, *Inorg. Chim. Acta*, 1987, **129**, 273–276.
41 For example, see: A. N. Dame, M. S. Bharara, C. L. Barnes and J. R. Walensky, *Eur. J. Inorg. Chem.*, 2015, 2996–3005.
42 For example, see: B. E. Klamm, C. J. Windorff, C. Celis-Barros, M. L. Marsh, D. S. Meeker and T. E. Albrecht-Schmitt, *Inorg. Chem.*, 2018, **57**, 15389–15398.
43 R. Selva Kumar, S. K. Ashok Kumar, K. Vijayakrishna, A. Sivaramakrishna, C. V. S. Brahmmananda Rao, N. Sivaraman and S. K. Sahoo, *Inorg. Chem.*, 2018, **57**, 15270–15279.
44 E. E. Hardy, K. M. Wyss, J. D. Gorden, I. R. Ariyarathna, E. Miliordos and A. E. V. Gorden, *Chem. Commun.*, 2017, **53**, 11984–11987.
45 D. F. Back, É. Bonfada, G. M. de Oliveira and E. S. Lang, *J. Inorg. Biochem.*, 2007, **101**, 709–714.
46 K. I. Alexopoulou, E. Zagoraiou, T. F. Zafiropoulos, C. P. Raptopoulou, V. Psycharis, A. Terzis and S. P. Perlepes, *Spectrochim. Acta, Part A*, 2015, **136**, 122–130.
47 A. Kagkelari, G. S. Papaefstathiou, C. P. Raptopoulou and T. F. Zafiropoulos, *Polyhedron*, 2009, **28**, 3279–3283.
48 K. I. Alexopoulou, A. Terzis, C. P. Raptopoulou, V. Psycharis, A. Escuer and S. P. Perlepes, *Inorg. Chem.*, 2015, **54**, 5615–5617.
49 P. S. Perlepe, A. A. Athanasopoulou, K. I. Alexopoulou, C. P. Raptopoulou, V. Psycharis, A. Escuer, S. P. Perlepes and T. C. Stamatatos, *Dalton Trans.*, 2014, **43**, 16605–16609.
50 For example, see: S. Dutta, P. Basu and A. Chakravorty, *Inorg. Chem.*, 1991, **30**, 4031–4037.
51 For example, see: R. Herchel, I. Nemec, M. Machata and Z. Trávniček, *Dalton Trans.*, 2016, **45**, 18622–18634.
52 N. C. Anastasiadis, D. A. Kalofolias, A. Philippidis, S. Tzani, C. P. Raptopoulou, V. Psycharis, C. J. Milios, A. Escuer and S. P. Perlepes, *Dalton Trans.*, 2015, **44**, 10200–10209.
53 E. C. Mazarakioti, L. Cunha-Silva, V. Bekiari, A. Escuer and T. C. Stamatatos, *RSC Adv.*, 2015, **5**, 92534–92538.
54 D. I. Alexandropoulos, T. N. Nguyen, L. Cunha-Silva, T. F. Zafiropoulos, A. Escuer, G. Christou and T. C. Stamatatos, *Inorg. Chem.*, 2013, **52**, 1179–1181.
55 S. T. Tsantis, V. Bekiari, C. P. Raptopoulou, D. I. Tzimopoulos, V. Psycharis and S. P. Perlepes, *Polyhedron*, 2018, **152**, 172–178.
56 S. T. Tsantis, M. Mouzakitis, A. Savvidou, C. P. Raptopoulou, V. Psycharis and S. P. Perlepes, *Inorg. Chem. Commun.*, 2015, **59**, 57–60.
57 S. T. Tsantis, E. Zagoraiou, A. Savvidou, C. P. Raptopoulou, V. Psycharis, L. Szyrwiel, M. Hołyńska and S. P. Perlepes, *Dalton Trans.*, 2016, **45**, 9307–9319.
58 E. Labisbal, L. Rodríguez, A. Vizoso, M. Alonso, J. Romero, J.-A. García-Vázquez, A. Sousa-Pedrares and A. Sousa, *Z. Anorg. Allg. Chem.*, 2005, **631**, 2107–2114.
59 Y. Elerman, A. Elmali, O. Atakol and I. Svoboda, *Acta Crystallogr., Sect. C: Cryst. Struct. Commun.*, 1995, **51**, 2344–2346.
60 D. Gürbüz, A. Cinarli, A. Tavman and A. S. Birteksz, *Chin. J. Chem.*, 2012, **30**, 970–978.
61 *CrystalClear*, Rigaku/MSC Inc., The Woodlands, TX, USA, 2005.
62 G. M. Sheldrick, *Acta Crystallogr., Sect. A: Found. Crystallogr.*, 2008, **64**, 112–122.
63 G. M. Sheldrick, *Acta Crystallogr., Sect. C: Struct. Chem.*, 2015, **71**, 3–8.
64 *DIAMOND: Crystal and Molecular Structure Visualization, Ver. 3.1*, Crystal Impact GbR, Bonn, Germany, 2011.
65 R. A. Coxall, S. G. Harris, D. K. Henderson, S. Parsons, P. A. Tasker and R. E. P. Winpenny, *J. Chem. Soc., Dalton Trans.*, 2000, 2349–2356.
66 M. Llunell, D. Casanova, J. Cirera, P. Alemany and S. Alvarez, *SHAPE, version 2.0*, Barcelona, Spain, 2010.
67 R. D. Rogers, A. H. Bond and M. M. Witt, *Inorg. Chim. Acta*, 1991, **182**, 9–17.
68 N. E. Travia, B. L. Scott and J. L. Kiplinger, *Chem. – Eur. J.*, 2014, **20**, 16846–16852.
69 R. Graziani, U. Casellato, P. A. Vigato, O. A. Rajan and A. Chakravorty, *Inorg. Chim. Acta*, 1981, **49**, 129–134.
70 S. T. Tsantis, C. P. Raptopoulou, D. I. Tzimopoulos, V. Psycharis and S. P. Perlepes, manuscript in preparation.
71 D. Maniaki, I. Mylonas-Margaritis, J. Mayans, A. Savvidou, C. P. Raptopoulou, V. Bekiari, V. Psycharis, A. Escuer and S. P. Perlepes, *Dalton Trans.*, 2018, **47**, 11859–11872.
72 E. C. Mazarakioti, A. S. Beobide, V. Angelidou, C. G. Efthymiou, A. Terzis, V. Psycharis, G. A. Voyiatzis and S. P. Perlepes, *Molecules*, 2019, **24**, 2219.

Open Access Article. Published on 02 2019. Downloaded on 2025/7/31 07:35:32.
This article is licensed under a Creative Commons Attribution 3.0 Unported Licence.

73 J. J. Lopez-Garriga, G. T. Babcock and J. F. Harrison, *J. Am. Chem. Soc.*, 1986, **108**, 7241–7251.
74 K. Nakamoto, *Infrared and Raman Spectra of Inorganic and Coordination Compounds*, Wiley, New York, 4th edn, 1986, pp. 254–257.
75 Z. G. Lada, A. S. Beobide, A. Savvidou, C. P. Raptopoulou, V. Psycharis, G. A. Voyiatzis, M. M. Turnbull and S. P. Perlepes, *Dalton Trans.*, 2017, **46**, 260–274.
76 F. R. Dollish, W. G. Fateley and F. F. Bentley, *Characteristic Raman Frequencies of Organic Compounds*, Wiley, New York, 1974, pp. 1–11, 134–142, 162–190.
77 W. G. Fateley, F. R. Dollish, N. T. McDerrit and F. F. Bentley, *Infrared and Raman Selection Rules for Molecular and Lattice Vibrations: The Corellation Method*, Wiley, New York, 1972, pp. 1–51.
78 W. J. Geary, *Coord. Chem. Rev.*, 1971, **7**, 81–122.
79 G. Knör and A. Strasser, *Inorg. Chem. Commun.*, 2002, **5**, 993–995.
80 H. Kunkely and A. Vogler, *Chem. Phys. Lett.*, 1999, **304**, 187–190.
81 B. A. Maynard, R. E. Sykora, J. T. Mague and A. E. V. Gorden, *Chem. Commun.*, 2010, **46**, 4944–4946.
82 J. Wen, L. Dong, J. Tian, T. Jiang, Y.-Q. Yang, Z. Huang, X.-Q. Yu, C.-W. Hu, S. Hu, T.-Z. Yang and X.-L. Wang, *J. Hazard. Mater.*, 2013, **263**, 638–642.
83 R. Gao, J. Hu, K. Zhang, Y. He, P. Liu, S. Luo, Y. Yang, L. Yang, W. Feng and L. Yuan, *Chin. J. Chem.*, 2013, **31**, 689–694.
84 J. Wen, L. Dong, S. Hu, W. Li, S. Li and X. Wang, *Chem. – Asian J.*, 2016, **11**, 49–53.
85 J. Du, D. M. King, L. Chatelain, E. Lu, F. Tuna, E. J. L. McInnes, A. J. Wooles, L. Maron and S. T. Liddle, *Chem. Sci.*, 2019, **10**, 3738–3745.
86 P. Farger, B. Haidon, P. Roussel, B. Arab-Chapelet and M. Rivenet, *Inorg. Chem.*, 2019, **58**, 1267–1277.
87 T. Cheisson, K. D. Kersey, N. Mahieu, A. McSkimming, M. R. Gau, P. J. Carroll and E. J. Schelter, *J. Am. Chem. Soc.*, 2019, **141**, 9185–9190.
88 C. Zhang, G. Hou, G. Zi and M. D. Walter, *Dalton Trans.*, 2019, **48**, 2377–2387.
89 D. N. Huh, S. Roy, J. W. Ziller, F. Furche and W. J. Evans, *J. Am. Chem. Soc.*, 2019, **141**, 12458–12463.
90 J. N. Wacker, M. Vasiliu, I. Colliard, R. L. Ayscue, III, S. Y. Han, J. A. Bertke, M. Nyman, D. A. Dixon and K. E. Knope, *Inorg. Chem.*, 2019, **58**, 10871–10882.
91 C. J. Inman and F. G. N. Cloke, *Dalton Trans.*, 2019, **48**, 10782–10784.
92 R. Selva Kumar and S. K. Ashok Kumar, *Dalton Trans.*, 2019, **48**, 12607–12614, and references cited therein.
93 J. A. Pool, B. L. Scott and J. L. Kiplinger, *Chem. Commun.*, 2005, 2591–2593.

This journal is © The Royal Society of Chemistry 2019